ARTICLE
Journal of Cellular Biochemistry 111:1501–1511 (2010)

Journal of Cellular Biochemistry

Betulinic Acid Inhibits High Glucose-Induced Vascular Smooth Muscle Cells Proliferation and Migration

Jung Joo Yoon,[1,2] Yun Jung Lee,[1,2] Jin Sook Kim,[3] Dae Gill Kang,[1,2*] and Ho Sub Lee[1,2*]

[1] *College of Oriental Medicine and Professional Graduate School of Oriental Medicine, Wonkwang University, Iksan, Chonbuk 570-749, Republic of Korea*

[2] *Hanbang Body-Fluid Research Center, Wonkwang University, Shinyong-dong, Iksan, Chonbuk 570-749, Republic of Korea*

[3] *Korea Institute of Oriental Medicine, Jeonmin-dong, Yusung-gu, Daejeon 305-811, Republic of Korea*

ABSTRACT

The proliferation of vascular smooth muscle cells may perform a crucial role in the pathogenesis of diabetic vascular disease. The principal objective of this study was to determine the effects of betulinic acid (BA) on human aortic smooth muscle cell (HASMC) proliferation induced by high glucose (HG). In this study, [^{3}H]-thymidine incorporation under 25 mM HG was accelerated significantly as compared with 5.5 mM glucose, and this increase was inhibited significantly by BA treatment. We utilized Western blotting analysis to evaluate the effects of BA on cell-cycle regulatory proteins. HG induced the expression of cyclins/CDKs and reduced the expression of $p21^{waf1/cip1}$/$p27^{kip1}$. However, BA also attenuated the expression of HG-induced cell-cycle regulatory proteins. The results of gelatin zymography demonstrated that the HG-treated HASMC secreted gelatinases, probably including MMP-2/-9, which may be involved in the invasion and migration of HASMC. Additionally, BA suppressed the protein and mRNA expression levels of MMP-2/-9 in a dose-dependent manner. BA inhibited the production of HG-induced hydrogen peroxide (H_2O_2) and the formation of DCF-sensitive intracellular reactive oxygen species (ROS). Further, BA suppressed the nuclear translocation and phosphorylation of IκB-α of NF-κB under HG conditions. Our results showed that BA exerts multiple effects on HG-induced HASMC proliferation and migration, including the inhibition of both MMP-2 and MMP-9 transcription, protein activity, and the downregulation of ROS/NF-κB signaling, thereby suggesting that BA may be a possible therapeutic approach to the inhibition of diabetic vascular disease. J. Cell. Biochem. 111: 1501–1511, 2010.

KEY WORDS: BETULINIC ACID; PROLIFERATION; MIGRATION; HIGH GLUCOSE; MMPs; HASMC

The fact that diabetic patients have an increased risk of atherosclerotic vascular disease has been well documented [Ruderman and Haudenschild, 1984; Ross, 1993]. The progression of atherosclerotic lesion or alteration of vasculature is the characteristic feature of diabetic complications. The proliferation and migration of vascular smooth muscle cells (VSMCs) from the tunica media to the subendothelial region are key events in the development, which play a crucial role in the degradation and remodeling of vascular basement membrane [Srivastava, 2002; Orr et al., 2005]. In many cells, transit through the G1 phase of the cell cycle and entry into the S-phase require the binding and activation of cyclin/CDK complexes, predominantly cyclin D1/CDK4 and cyclin E/CDK2 [Sherr, 1996]. The kinase activities of the cyclin/CDK complexes are known to be negatively regulated by CDK inhibitors, including $p21^{waf1/cip1}$ and $p27^{kip1}$ [Suh et al., 2006]. In recent years, it has become clear that chronic hyperglycemia enhances VSMC proliferation and migration [Yasunari et al., 1997; Maile et al., 2007].

Increased proteolytic activity in the vessel wall mediates the degradation of the extracellular matrix surrounding the VSMC in response to injury. The activation of matrix metalloproteinase (MMP) may contribute to the pathogenesis of atherosclerosis by facilitating the migration of VSMC [Shah, 1998]. Analyses of human atherosclerotic lesions and advanced plaques are indicative of increased MMP expression, especially the gelatinases MMP-2 and MMP-9, occurring predominantly in the VSMC. Oxidative injury

Additional Supporting Information may be found in the online version of this article.

Grant sponsor: Ministry of Education, Science and Technology (MEST); Grant number: R13-2008-028-01000-0; Grant sponsor: Korea Institute of Oriental Medicine; Grant number: K10040.

*Correspondence to: Dr. Dae Gill Kang and Ho Sub Lee, College of Oriental Medicine and Professional Graduate School of Oriental Medicine, Wonkwang University, Iksan, Chonbuk 570-749, Republic of Korea. E-mail: dgkang@wku.ac.kr; host@wku.ac.kr

Received 17 February 2010; Accepted 1 September 2010 • DOI 10.1002/jcb.22880 • © 2010 Wiley-Liss, Inc.
Published online 24 September 2010 in Wiley Online Library (wileyonlinelibrary.com).

due to high glucose (HG) concentrations performs a central role in the development of diabetic complications [Piconi et al., 2004]. It may trigger many cellular events, including the inactivation of NO, enhanced mitogenicity, and vascular cell apoptosis [Wassmann et al., 2006]. Furthermore, oxidative stress can also activate or increase the expression of redox-sensitive genes, including those that code for the adhesion molecules and cell-cycle progression regulators, NF-κB and MMP [De Martin et al., 2000].

Natural products derived from plant resources have been extensively utilized in traditional medicine for the treatment of vascular disorders such as stroke or atherosclerosis. The Labiatae plant, *Lycopus lucidus* TURCZ, is a perennial herb that is distributed broadly throughout Korea and China [Kwon et al., 2002; Yoon et al., 2010]. Betulinic acid (BA), a pentacyclic triterpene isolated from *L. lucidus*, has been reported to exert a variety of biological effects, including anti-neoplastic activity in several human cancer cells, as well as anti-HIV, anti-inflammatory, and immunomodulatory properties [Kwon et al., 2002]. We reported previously that BA evidences an anti-inflammatory property in vascular endothelial cells [Yoon et al., 2010]. However, the mechanisms underlying the inhibitory effects of BA in VSMC proliferation remain to be clearly elucidated. Thus, the principal objective of this study was to compare the proliferation of human aortic smooth muscle cells (HASMC) in a medium containing a physiologically normal glucose level and one containing a HG level, and to evaluate the anti-proliferative effects of BA in HG-induced changes in HASMC proliferation.

MATERIALS AND METHODS

MATERIALS

BA (Fig. 1A) and Bay 11-7082 were purchased from Calbiochem (San Diego, CA). D-Glucose, gelatin, *N*-acetyl cysteine (NAC), and pyrrolidine dithiocarbamate (PDTC) were purchased from Sigma Chemical Company (St. Louis, MO). CM-H_2DCFDA was purchased from Invitrogen, Inc. (Carlsbad, CA). Mouse monoclonal antibodies to cyclins, $p27^{kip1}$, β-actin, and MMPs were obtained from Santa Cruz Biotechnology (Santa Cruz, CA). Rabbit polyclonal antibodies to CDKs, $p21^{waf1/cip1}$, NF-κB p65, phopho IκB-α, IκB-α, MMP-2, and MMP-9 were purchased from Santa Cruz Biotechnology. Goat anti-rabbit IgG and goat anti-mouse IgG were purchased from Jackson Immunoresearch (West Grove, PA), and all other reagents were of the highest commercially available purity.

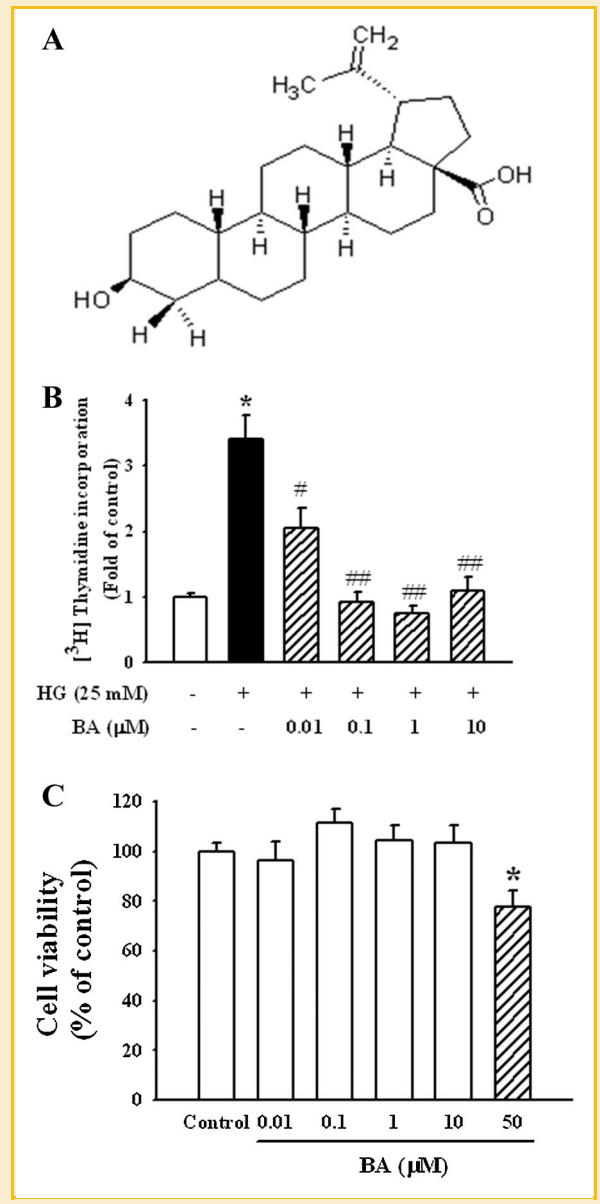

Fig. 1. Effect of BA on HG-induced HASMC proliferation. A: Chemical structure of BA. B: HASMC were pretreated with BA (0–10 μM) for 30 min prior to the treatment of 25 mM glucose (HG) for 24 h. C: The effect of BA on cytotoxicity. HASMC were treated with various concentration (0–50 μM) of BA for 48 h. $^{*}P < 0.01$ versus control, $^{\#}<0.05$, $^{\#\#}<0.01$ versus HG alone.

CELL CULTURE AND VIABILITY TEST

Primary cultured HASMC (#C-007-5C), medium 231, and smooth muscle growth supplements were purchased from Invitrogen, Inc., which contains fetal bovine serum (5%, v/v, final concentration), recombinant human basic fibroblast growth factor, recombinant human epidermal growth factor, insulin, etc. HASMC, plated at 4×10^4/well and used between passages 3 and 8, were maintained in a humidified chamber containing 5% CO_2 at 37°C. To determine HASMC viability exposure to BA, 3-(4,5-dimethylthiazol-2-yl)-2,5-diphenyltetrazolium bromide (MTT, 0.5 mg) was added to 1 ml of cell suspension for 4 h. After three washes of cells with PBS, the insoluble formazan product was dissolved in DMSO. Optical density of each culture well was measured using microplate reader at 590 nm (Multiskan, Thermo Labsystems, Inc., Franklin, MA). The optical density in control cells was taken as 100% of viability.

CELL PROLIFERATION

[^{3}H]-Thymidine incorporation was assessed in order to determine its effects on HASMC cell proliferation [Gabelman and Emerman, 1992]. Quiescent cells were treated with 25 mM glucose and BA, respectively, and 1 μCi of [^{3}H]-thymidine was added (methyl-[^{3}H] thymidine, 50 Ci/mmol; Amersham, Oakville, Ontario, Canada). After 24 h of incubation, cells were washed once with 2 ml of

ice-cold PBS for 10 min, extracted three times with 2 ml of cold 10% TCA for 5 min each, and solubilized for at least 30 min at room temperature in 0.2 ml of 0.3 N NaOH, 1% SDS. After neutralization with 0.2 ml of 0.3 N HCl, [^{3}H]-thymidine activity was measured in a liquid scintillation counter (Beckman LS 7500, Fullerton, CA). Each experiment was conducted either in triplicate or quadruplicate.

BASEMENT MEMBRANE INVASION ASSAY USING MATRIGEL

Matrigel-coated filter inserts (8 μm pore size) that fit into 24-well invasion chambers were obtained from BD BioCoat™ (San Diego, CA). Invasion chambers were used for monitoring cell invasion as described previously [Ramos-DeSimone et al., 1999]. Cells were seeded onto the upper transwell chamber, and the lower chamber contained the experimental reagents. The chambers were incubated for 24 h at 37°C in 5% CO_2. After incubation, the inserts were removed and the cells on the upper side of the filter were removed with cotton swabs. The filters were fixed, stained, and mounted. The number of migrated cells was determined by counting the number of stained cells. The microscopic photographs of invasion were produced via fluorescence microscopy (Axiovision 4, Zeiss, Germany). Three to five chambers were utilized per condition. The obtained values were calculated by averaging cell numbers from three filters.

MIGRATION ASSAY

The effect of BA on the migration of HASMC was evaluated via a wound-healing assay. In brief, HASMC were grown to confluence in six-well culture plates. A scratch was made using a yellow tip, after which the HASMC were incubated for 24 h with or without HG (25 mM) and various concentrations of BA in serum-free media. After 24 h of incubation, the cells were washed three times with ice-cold PBS. The cells were then fixed with methyl alcohol for 5 min and stained with hematoxylin and eosin. The microscopic photographs of migrated cells were generated via fluorescence microscopy (DMIRB, Leica, Germany). In each group, three duplicate wells were assayed, and each assay was conducted at least in triplicate.

WESTERN BLOT ANALYSIS

Cell homogenates (40 μg of protein) were separated on 10% SDS–polyacrylamide gel electrophoresis and transferred to nitrocellulose paper. The blots were then washed with H_2O, blocked with 5% skimmed milk powder in TBST [10 mM Tris–HCl (pH 7.6), 150 mM NaCl, 0.05% Tween-20] for 1 h and incubated with the appropriate primary antibody at dilutions recommended by the supplier. The membrane was then washed, and primary antibodies were detected with goat anti-rabbit-IgG conjugated to horseradish peroxidase, and the bands were visualized with enhanced chemiluminescence (Amersham, Buckinghamshire, UK). Protein expression levels were determined by analyzing the signals captured on the nitrocellulose membranes using a Chemi-doc image analyzer (Bio-Rad, Inc., Hercules, CA).

MRNA ISOLATION AND REAL-TIME QRT-PCR

A kit from Qiagene (RNeasy™ Plus mini kit) was utilized for mRNA isolation from cell cultures, and RNA quality was evaluated by measuring the 260/280 nm ratio in a UV-spectrophotometer. Real-time quantitative RT-PCR analysis was conducted in 48-well plates using the Opticon MJ Research instrument (Bio-Rad, Inc.) and optimized with a standard SYBR Green 2-step qRT-PCR kit (DyNAmo™, Finnzymes, Finland). Specific sense and anti-sense primers used were as follows: MMP-2, 231 bp, sense: 5′-CAA-AAACAAGAAGACATACAT-3′, anti-sense: 5′-GCTTCCAAACTT-CACGCTC-3′; MMP-9, 223 bp, sense: 5′-TGGGGGGCAACTCGGC-3′, anti-sense: 5′-GGAATGATCTAAGCCCAG-3′. PCR was initiated at 95°C for 15 min (hot start) to activate AmpliTaq polymerase, followed by a 45-cycle amplification (denaturation at 94°C for 20 s, annealing at 60°C for 30 s, extension at 72°C for 60 s, and plate reading at 60°C for 10 s). The temperature of the PCR products was raised from 65 to 95°C at a rate of 0.2°C/1 s, and the resultant data were analyzed using the software provided by the manufacturer.

GELATIN ZYMOGRAPHY

MMP-2 and MMP-9 enzymatic activities were assayed by gelatin zymography [Herron et al., 1986]. Samples were electrophoresed on 1 mg/ml gelatin containing 10% SDS–polyacrylamide gel. After electrophoresis, the gel was washed twice with washing buffer (50 mM Tris–HCl, pH 7.5, 100 mM NaCl, 2.5% Triton X-100), followed by a brief rinsing in washing buffer without Triton X-100. The gel was incubated with incubation buffer (50 mM Tris–HCl, pH 7.5, 150 mM NaCl, 10 mM $CaCl_2$, 0.02% NaN_3, 1 μM $ZnCl_2$) at 37°C. After incubation, the gel was stained with Coomassie brilliant blue R-250 and destained. A clear zone of gelatin digestion was represented with the MMP activity.

INTRACELLULAR ROS PRODUCTION ASSAY

The fluorescent probe, CM-H_2DCFDA, was used to determine the intracellular generation of ROS by HG, as described elsewhere [Liu et al., 2004]. Briefly, the confluent HASMC in the 24-well culture plates were pretreated with BA for 1 h. After removing the BA from the wells, HASMC were incubated with 20 μM CM-H_2DCFDA for 1 h. The HASMC were then stimulated with TNF-α, and the fluorescence intensity (relative fluorescence units) was measured by flow cytometry on FACScalibur (BD) and spectrofluorometer at an excitation and emission wavelength of 485 and 530 nm, respectively.

H_2O_2 RELEASE ASSAY

Extracellular H_2O_2 production was quantified using the Amplex Red Hydrogen Peroxide Assay Kit (Molecular Probes, Eugene, OR) according to manufacturer's recommendation. The cells washed twice with ice-cold PBS and were harvested cells by microcentrifugation and resuspended in a Krebs-Ringer phosphate (KRPG) solution. One hundred microliter of the reaction mixture (50 μM Amplex Red reagent containing 0.1 U/ml HRP in KRPG) was added into each microplate well and then prewarm at 37°C for 10 min. After then, the reaction was started as adding resuspended cells in 20 μl of KRPG. Fluorescence readings became stable within 30 min of starting of reaction equipped for absorbance at ~560 nm

(Multiskan, Thermo Labsystems, Inc.). A reagent H_2O_2 standard curve was used to calculate H_2O_2 concentration.

IMMUNOFLUORESCENCE MICROSCOPY

HASMC were fixed with 4% paraformaldehyde for 30 min at room temperature. It was permeabilized by treatment with 0.1% Triton X-100 for 30 min at room temperature. The cells were overlaid with protease-free BSA for 10 min, rinsed with PBS, and incubated with primary antibodies (p65 NF-κB, 1:100 in PBS) in a humid chamber overnight at 4°C. They were gently washed several times with PBS before incubation with secondary antibody goat-anti-rabbit IgG conjugated with FITC, 1:128 in PBS) for 2 h. Cells were finally washed three times with PBS, coverslips were mounted with Dako Fluorescent mounting medium onto the glass slides, and examined under a fluorescence microscope (Axiovision 4, Zeiss).

STATISTICAL ANALYSIS

All the experiments were repeated at least three times. The results were expressed as a mean ± SE, and the data were analyzed using one-way ANOVA followed by a Dunnett's test or Student's *t*-test to determine any significant differences. $P < 0.05$ was considered as statistically significance.

RESULT

EFFECT OF BA ON HG-INDUCED HASMC PROLIFERATION

In the experiment to determine the effect of HG (25 mM) on HASMC proliferation, we evaluated cell proliferation using [^{3}H]-thymidine incorporation. As shown in Figure 1A, the exposure of the HASMC to HG for 24 h induced cell proliferation ($P < 0.01$). However, the increase in [^{3}H]-thymidine incorporation induced by HG was reduced significantly as the result of pretreatment with 0.01–10 μM BA (Fig. 1B). In order to determine the effects of HG on the cell-cycle proteins, different BA doses were added to the HASMC and were examined by Western blotting. HG significantly increased the levels of cyclin D1/E and CDK2/4 expression in a dose-dependent manner. In contrast, HG levels resulted in a reduction in the levels of $p21^{waf1/cip1}$/$p27^{kip1}$, and CDK inhibitory protein (Fig. 2). BA pretreatment attenuated the HG-induced increases in cyclin D1/E, CDK2/4 and the decrease in $p21^{waf1/cip1}$/$p27^{kip1}$ expression levels. BA alone did not adversely affect the cell viability up to 50 μM

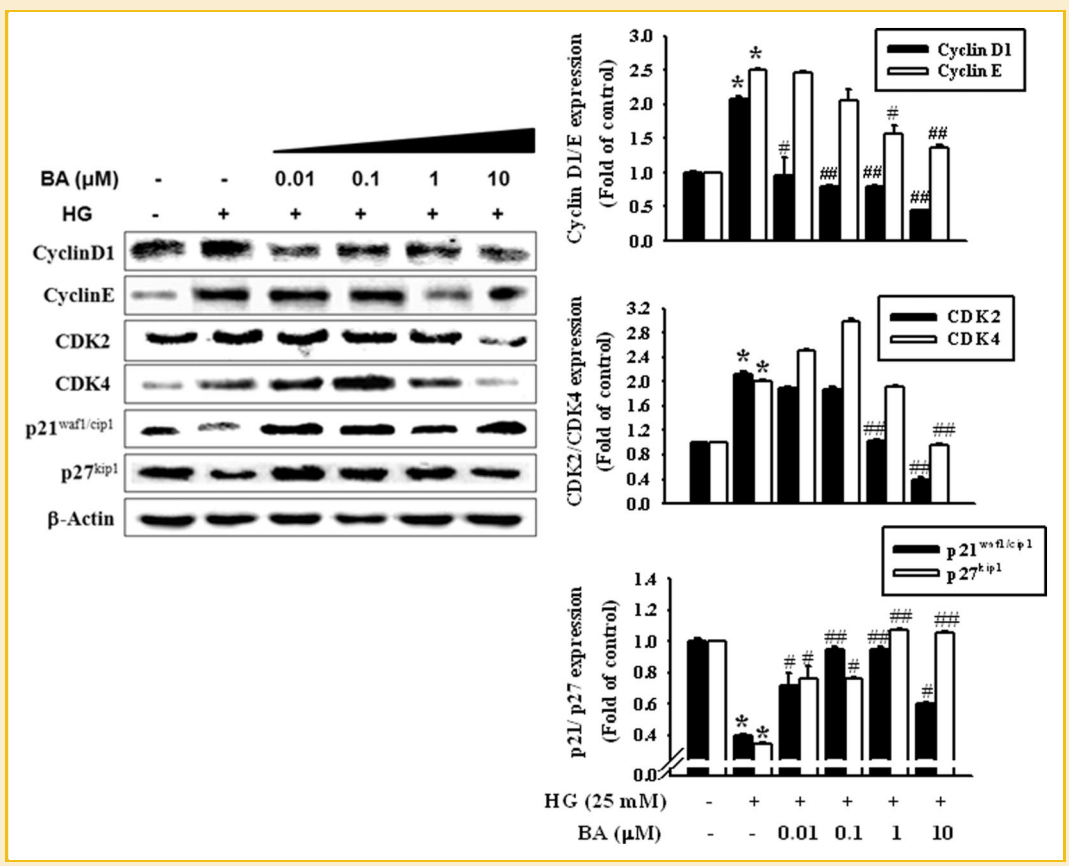

Fig. 2. The effect of BA on cell-cycle-related protein expression. HASMC were stimulated with HG in the presence or absence of indicated concentration of BA at 24 h and Western blot analysis was performed with specific antibodies. The data are expressed as a fold of basal value and are the means ± SE of five independent experiments with four dishes. $^{*}P < 0.01$ versus control, $^{\#} < 0.05$, $^{\#\#} < 0.01$ versus HG alone.

(Fig. 1C). Therefore, we confirmed that the concentration of BA did not result in cytotoxicity in the present study.

EFFECTS OF BA ON HG-INDUCED HASMC INVASION AND MIGRATION

Biological activity associated with MMP upregulation in HASMC was examined using an invasion assay using a BD Matrigel™ Invasion Chamber. HASMC were treated for 24 h with or without the indicated concentration of BA under HG condition. As shown in Figure 3A, HASMC which migrated to the lower chamber were also visualized under a fluorescence microscope. The migration of HASMC was significantly promoted by treatment with HG as compared with control. However, BA inhibited the HG-induced HASMC invasion in a dose-dependent manner ($P < 0.01$). In addition, as a separate assessment of HASMC cell migration, a wound-healing assay was performed in which the rate of wound closure (initial width 1 mm) was measured in confluent cell monolayers. The wounds healed linearly over 24 h in the HG-treated cells. However, the speed of the wound edge was decreased significantly in a dose-dependent manner in the BA pretreatment group (Fig. 3B). These results indicated that BA may perform an MMP-inhibitory role in the process of HASMC invasion into a "thick" matrix layer.

EFFECT OF BA ON HG-INDUCED INCREASE OF MMP-2 AND MMP-9

Since both MMP-2 and MMP-9 have been closely correlated with smooth muscle cell proliferation of vascular lesions and are activated by oxidative stress, HG-induced MMP-2 and MMP-9 expression and activity were examined. Western blotting showed that HG resulted in increases in the expression of both MMP-2 and MMP-9. The results of gelatin zymography also demonstrated that, in a HG culture medium, both MMP-2 and MMP-9 proteolytic activity were increased. BA pretreatment resulted in reduced MMP-2 and MMP-9 expression and proteolytic activity (Fig. 4A,B). Additionally, real-time qRT-PCR showed that HG-induced increases in MMP-2 and MMP-9 mRNA expression were reduced by BA pretreatment (Fig. 4C). We also attempted to determine whether BA could suppress the MMP-9 promoter in HASMC. Transient transfection was conducted using the MMP-9-dependent luciferase reporter plasmid in order to further evaluate the effects of BA on

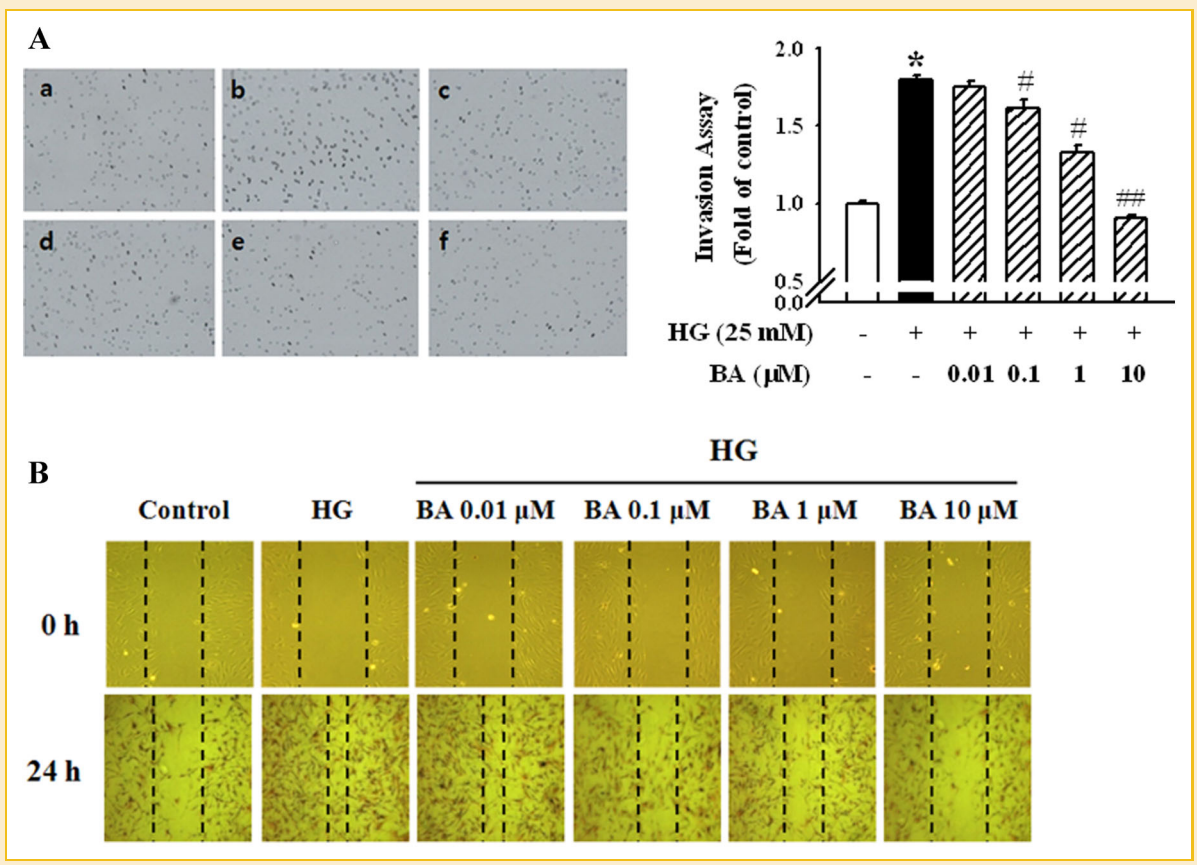

Fig. 3. Effect of BA on HG-induced HASMC invasion and migration. A: BA-treated HASMC were allowed to migrate on Matrigel matrix-coated transwell inserts for 24 h, stained and photographed. a: Control; (b) HG; (c) HG with BA (0.01 μM); (d) HG with BA (0.1 μM); (e) HG with BA (1 μM); (f) HG with BA (10 μM). Right panel indicated the fold value of cell invasion. Results are expressed as the mean ± SE from three independent experiments. $^{*}P < 0.01$ versus control, $^{\#\#}<0.01$ versus HG alone. B: Representative migration images showing HASMC cultures immediately after 0 h (upper) or 24 h (bottom) after scratch. HASMC were pretreated with BA (0–10 μM) for 30 min prior to the treatment of HG for 24 h. Dashed lines indicate wound edges. Each photograph is representative of the results from five independent experiments. [Color figure can be viewed in the online issue, which is available at wileyonlinelibrary.com.]

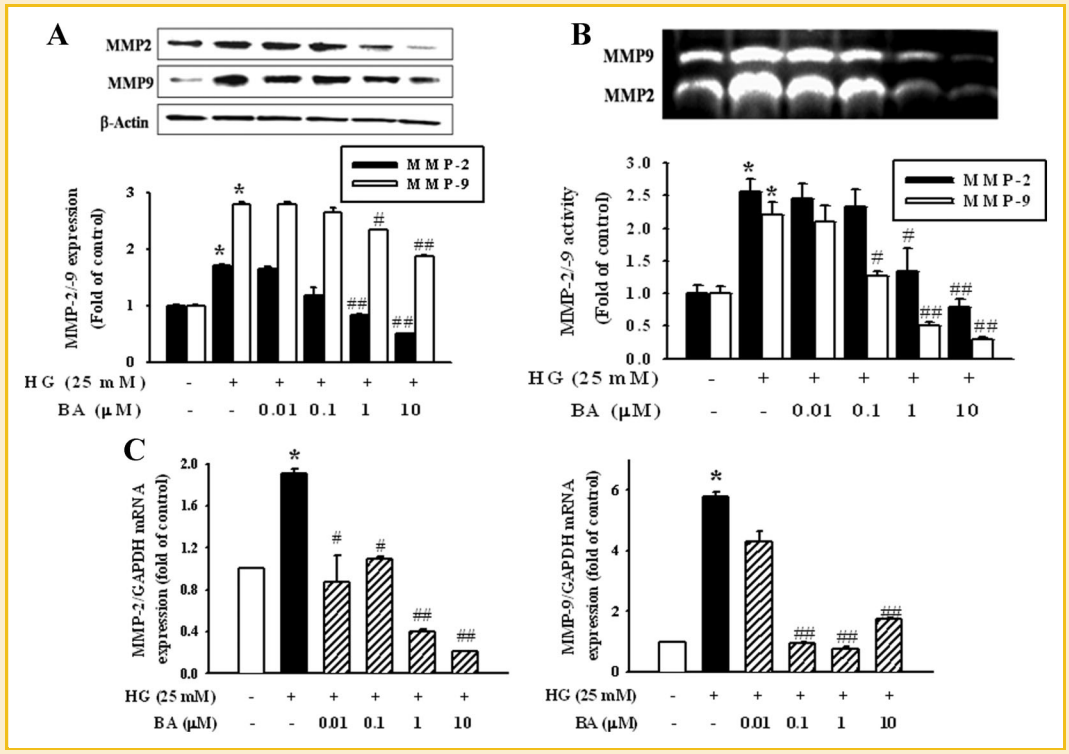

Fig. 4. Effect of BA on HG-induced MMP-2 and MMP-9 activity. A: HASMC were pretreated with BA (0–10 μM) for 30 min and then stimulated with HG for 24 h. The cell lysates were evaluated for MMP-2/-9 expression via Western blotting. B: The proteolytic activity of MMP-2/-9 in conditioned medium was analyzed by gelatin zymography. The results are expressed as the fold of the control and each electrophoretogram is representative of the results from five independent experiments. C: Real-time qRT-PCR analysis was performed using specific primer for MMP-2, MMP-9, and GAPDH, respectively. The data are expressed as a fold of basal value and are the means ± SE of five independent experiments with four dishes. $^{*}P < 0.01$ versus control, $^{\#} < 0.05$, $^{\#\#} < 0.01$ versus HG alone.

MMP-9 transcription activity. HG levels resulted in increased MMP-9 transcription activity, and 1 μM BA significantly inhibited HG-induced MMP-9 transcriptional activity (Supplementary Material 1).

INVOLVEMENT OF ROS IN INHIBITORY EFFECT OF BA ON HG-INDUCED HASMC PROLIFERATION

ROS has been shown to activate a variety of transcription factors as a common second messenger in a number of pathways that lead to NF-κB activation. Therefore, the level of intracellular ROS production was assessed by monitoring the fluorescence in order to determine whether BA can reduce the level of HG-induced oxidative stress in HASMC. As shown in Figure 5A, the degree of cellular hydrogen peroxide (H_2O_2) is increased with HG (25 mM) treatment. However, BA inhibited the HG-induced augmentation of H_2O_2. Additionally, DCF-DA fluorescence was increased significantly after incubation with HG, thereby suggesting that DCF-DA-sensitive ROS was generated in the HASMC (Fig. 5B). BA pretreatment prevented the HG-induced production of intracellular ROS. Figure 5C shows the antioxidant effects of BA on HG-induced ROS production as assessed by fluorescence-activated cell sorting analysis. BA reduced HG-induced ROS formation and NAC (50 μM) was used as a positive control.

INVOLVEMENT OF NF-*K*B IN INHIBITORY EFFECT OF BA ON HG-INDUCED HASMC PROLIFERATION

When cells are stimulated by HG, NF-κB is activated via the stimulated phosphorylation and degradation of IκB-α. The activated NF-κB is then translocated into the nucleus, resulting in the transcriptional expression of genes associated with cellular growth properties [Yokoo and Kitamura, 1996]. As shown in Figure 6A, HG induced NF-κB p65 nuclear translocation in the nucleus, which is inhibited by pretreatment with BA. HG-induced HASMC markedly decreased IκB-α expression level and increased phospho-IκB-α expression level. However, BA prevented the phosphorylation of IκB-α. These results suggested that BA inhibited both NF-κB activation and IκB-α degradation. Nuclear translocation of p65 NF-κB was also determined by immunocytochemical analyses as shown in Figure 6B. HASMC cultured in HG resulted in an increase in p65 NF-κB nuclear translocation as demonstrated by the intense green fluorescence localized within the nuclei of HASMC, and also from merged photomicrographs of DAPI-stained nuclei (Blue) with green fluorescence. Stimulation with HG profoundly increased the number of nuclei for the p65 NF-κB, whereas only a few p65 NF-κB nuclei could be detected in the presence of BA.

Next, we used BAY 11-7082 and PDTC to confirm the linkage NF-κB with MMP-2/9 or cell-cycle proteins. Bay 11-7082, an irreversible inhibitor of IkappaB-alpha phosphorylation, and PDTC,

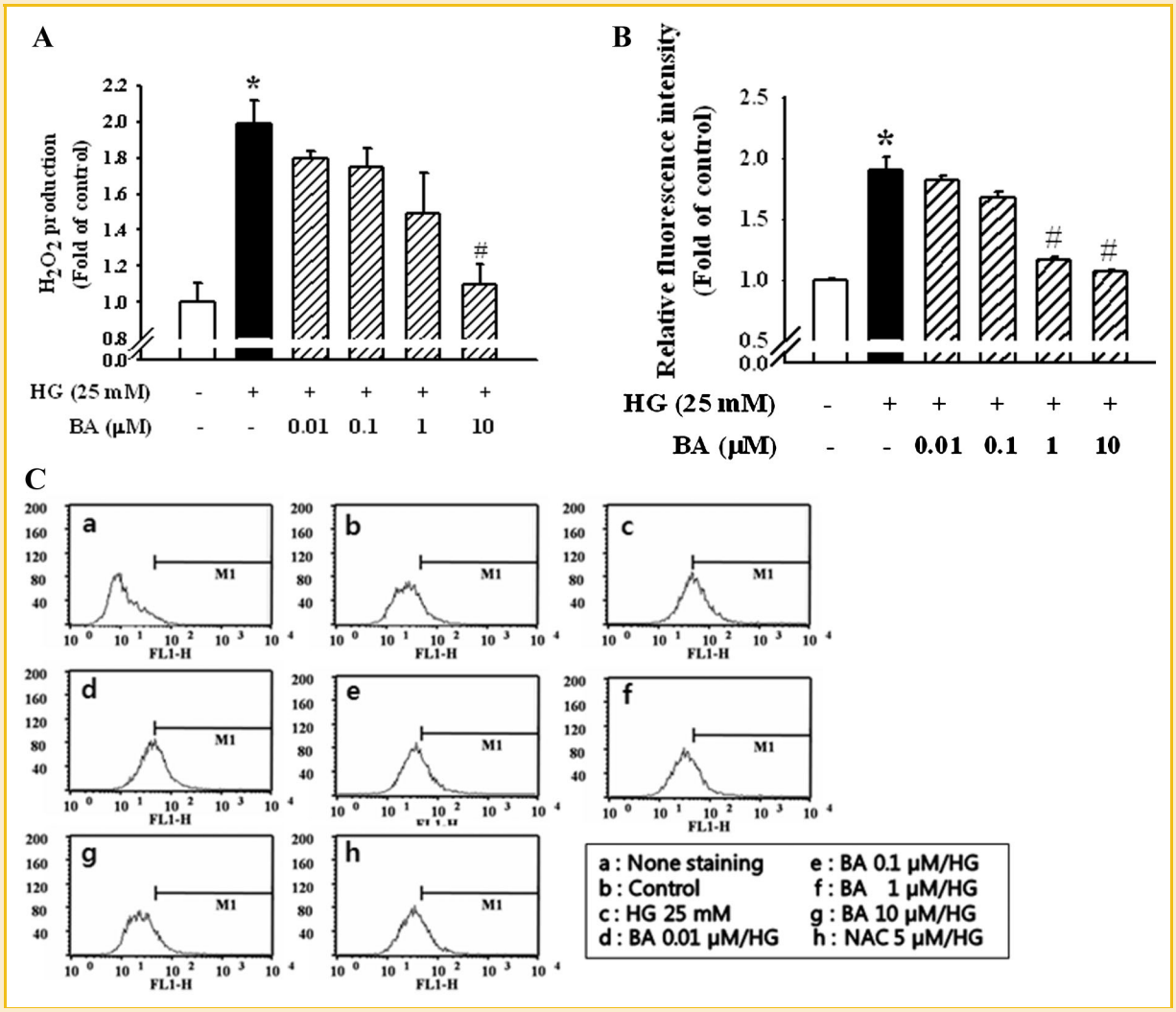

Fig. 5. Effect of BA on HG-induced intracellular ROS production. HASMC were pretreated with BA (0–10 μM) for 30 min and stimulated with HG for 1 h. DCF-sensitive ROS (A) and H_2O_2 assay (B) were measured on fluorescence microplates, and the relative ROS levels were quantified. The results are expressed as a fold of the fluorescence intensity ± SE of five individual experiments with triplicate dishes. C: FACS analysis on BA-induced antioxidant effect. $^{*}P < 0.01$ versus control, $^{\#}<0.05$, $^{\#\#}<0.01$ versus HG alone.

the potent NF-κB inhibitor, were used for inhibition of NF-κB pathway. Figure 7A showed that 1 μM Bay 11-7082 and 0.1–1 μM PDTC prevented HG-induced CDK2 and CDK4 expression in HASMC. Cyclin D1 and cyclin E also were prevented by Bay 11-7082 and PDTC (Fig. 7B). Pretreatment of Bay 11-7082 and PDTC inhibited HG-induced MMP-2/-9 expression, suggesting a role of NF-κB pathway in high glucose-induced gelatinase activation in HASMC (Fig. 7C). These results suggested that high glucose increase HASMC proliferation throughout activation of NF-κB.

DISCUSSION

Patients with diabetes are at higher risk for atherosclerotic disease than nondiabetic individuals with other comparable risk factors. The proliferation and migration of HASMC play important roles in atherosclerosis during the processes inherent to vascular disease [Yasunari et al., 1997; Suh et al., 2006]. Our study demonstrated that: (1) BA, at a nontoxic dose, inhibited HG-induced HASMC proliferation and migration in vitro; (2) BA directly inhibited both MMP-2 and MMP-9 proteolytic activity and expression under HG conditions in a dose-dependent manner; (3) BA inhibited HG-induced HASMC proliferation and migration, which may be closely related with the downregulation of ROS/NF-κB signaling. Our results are, to the best of our knowledge, the first evidence to suggest that BA exerts multiple effects in the inhibition of HASMC proliferation, suggesting that the downregulation of MMP-2 and MMP-9 activity and/or the inhibition of ROS production and/or NF-κB activation may offer a therapeutic approach for the blockage of diabetic atherosclerosis.

In this study, [^{3}H]-thymidine incorporation as an index of DNA synthesis showed that BA resulted in G1 cell-cycle arrest in HASMC. Our Western blotting results also showed that pretreatment of HASMC with BA resulted in significant downmodulation of all these

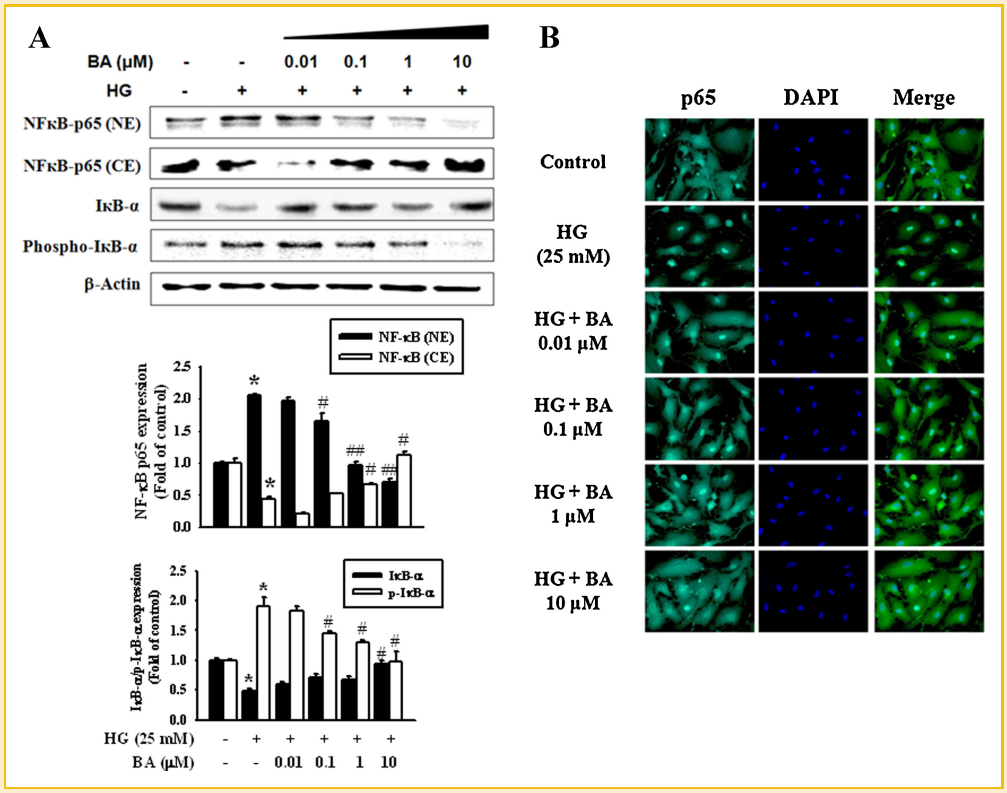

Fig. 6. Effect of BA on HG-induced NF-κB p65 expression in HASMC. Cells were treated with the indicated concentrations of BA for 24 h. A: Nuclear extracts and cytoplasmic extracts were subjected to Western blotting to detect NF-κB p65 and phospho IκB-α levels using a specific antibody. Each value represents the means ± SE of three independent experiments. $^{**}P < 0.01$ $^{*}P < 0.05$ versus control, $^{\#\#}<0.01$, $^{\#}< 0.05$ versus HG alone. B: BA reduces HG-induced nuclear translocation of NF-κB p65 subunit. Localization of NF-κB p65 immunostaining using a monoclonal antibody against the p65 subunit (green fluorescence), nuclei stained with DAPI (Blue), and composite images generated by superimposing photographs. Each photograph is representative of the results from five independent experiments. [Color figure can be viewed in the online issue, which is available at wileyonlinelibrary.com.]

regulatory molecules in the G1-phase of the cell cycle—specifically, cyclin D1, cyclin E, CDK2, and CDK4. $p21^{waf1/cip1}$ and $p27^{kip1}$ are regarded as universal inhibitors of the cyclin/CDK complexes [Sherr, 1996; Suh et al., 2006]. BA pretreatment attenuated the HG-induced increases of $p21^{waf1/cip1}$ and $p27^{kip1}$ expressions, thereby suggesting that BA may also be responsible for the G1-phase arrest of HASMC under HG conditions.

We determined that BA induced a marked inhibition of HG-induced HASMC migration and also inhibited the activities of MMP-2 and MMP-9. This effect was not likely caused by drug toxicity, as the MTT assay results demonstrated no differences in cytotoxicity between the BA-treated and control HASMC cultures. Similar results were obtained when minocycline, a widely used antibiotic, significantly reduced HASMC migration without cytotoxicity after vascular endothelial growth factor treatment [Yao et al., 2004]. These findings extend our recent discovery showing that pretreatment with BA, at nontoxic doses, reduces the migration speed of HASMC in vitro.

VSMC migration presumably requires degradation of the basement membrane and extracellular matrix surrounding the cell. Many studies have identified increased MMP-2 and MMP-9 expression, coinciding with VSMC migration after vascular injury in vitro and in vivo [Lee et al., 2006; Lin et al., 2007]. MMP-2 and MMP-9 perform pivotal roles in the proliferation of HASMC, and the inhibition of their expression is clearly relevant to the search for natural therapeutic herbs. The results of gelatin zymography and Western blotting revealed that pretreatment with BA reduced the levels of HG-induced MMP-2 and MMP-9 activity and expression in a dose-dependent manner. MMP-2 and MMP-9 mRNA expression also increased by HG and pretreatment with BA inhibited mRNA expression. This result indicated that pretreatment with BA reduced HG-induced MMP-2 and MMP-9 proteolytic activity and transcriptional activity in a dose-dependent manner, possibly reflecting an anti-atherosclerotic role of BA.

Although MMP-2 and MMP-9 have similar substrate specificities, the regulation of their expression is different [Jin et al., 2008]. MMP-2 is constitutively expressed in VSMC, and neither cytokines nor growth factors could induce its expression [Fabunmi et al., 1996]. By way of contrast, the basal levels of MMP-9 in VSMC are generally low, and cytokines or growth factors could induce its expression [Jiang et al., 2009]. Several reports have demonstrated that MMP-9 is stronger than MMP-2 in the pathogenesis of a variety of diseases [Xu et al., 2000; Matsumoto et al., 2009]. Interestingly, in our experiment, BA was shown to inhibit both MMP-2 and MMP-9 activities, possibly via the direct or indirect downregulation of gelatinases followed by the inhibition of VSMC migration. The mechanisms by which BA inhibits HG-induced HASMC migration remain to be thoroughly elucidated. One potential explanation for

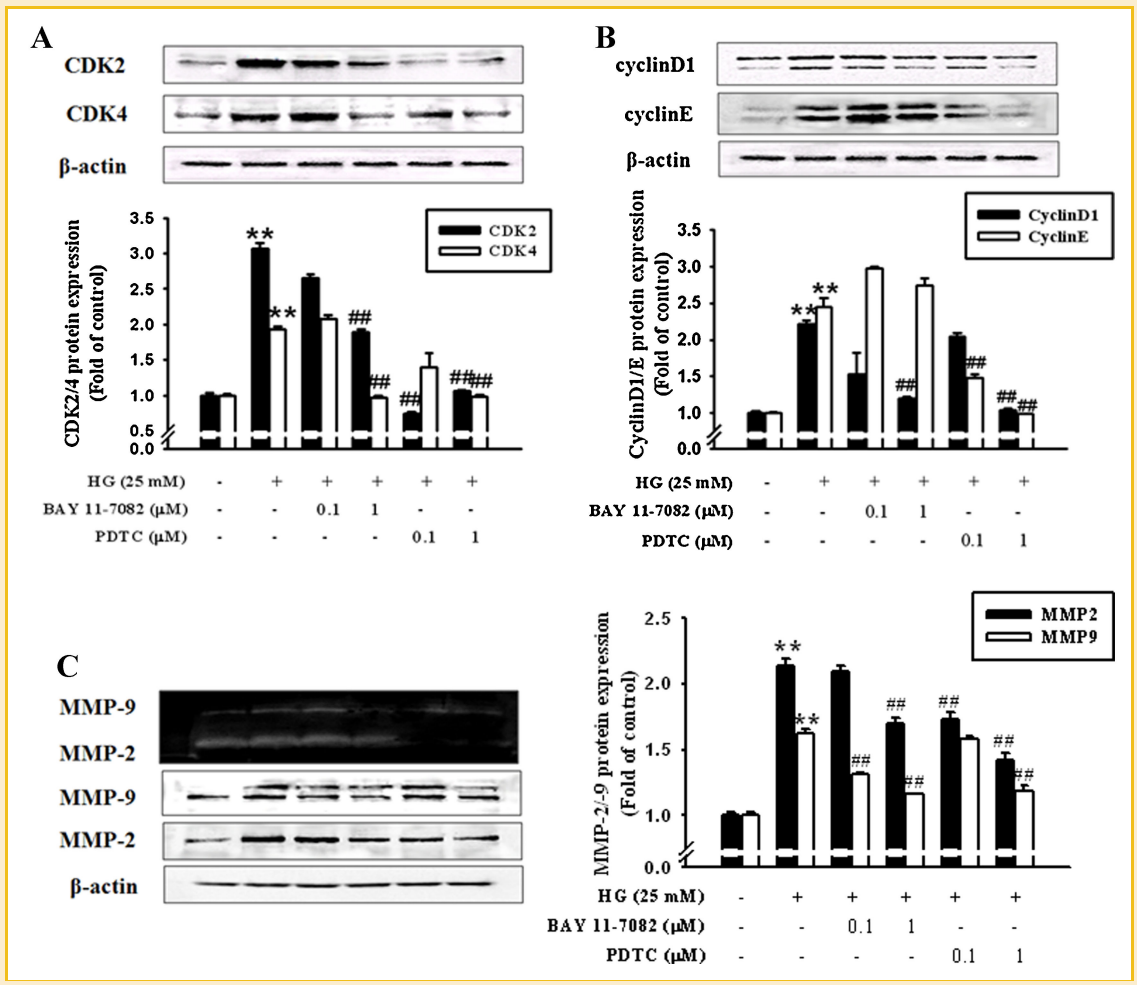

Fig. 7. Effect of Bay 11-7082 and PDTC on HG-induced cell cycle and gelatinase expression. Cells were pretreated with the indicated concentrations of Bay 11-7082 or PDTC for 30 min prior to the treatment with HG. Western blot analysis was performed with CDK2 and CDK4 (A), cyclin D1 and cyclin E (B). Zymography and Western blot analysis were performed with MMP-2/MMP-9 (C). Each value represents the means ± SE of three independent experiments. $^{**}P < 0.01$ versus control, $^{\#\#} < 0.01$ versus HG alone.

this is thought to be the downregulation of both MMP-2 and MMP-9 activities, a process that occurs via both direct and indirect mechanisms. One possible inhibitory mechanism of BA involves the blockage of the active sites of MMPs or the induction of conformational changes that render the proenzyme susceptible to fragmentation during activation [Golub et al., 1998; Burggraf et al., 2007]. Another possibility is that BA prevents pro-MMP-2 and pro-MMP-9 activation via the inhibition of endogenous activators such as membrane-type (MT)1–MMP or ROS [Jo et al., 2004; Park et al., 2007]. Here, we began with the suspicion that the BA-induced downregulation of gelatinases is regulated by the antioxidant effect of BA itself.

Excess ROS accumulation has been previously reported in both human and rodent diabetic vessels. ROS has also been confidently associated with excess VSMC proliferation, via the activation of MAPKs and transcription factors [Wassmann et al., 2006]. Both MMP-2 and MMP-9 can be activated by ROS, and their expression appears to be regulated by oxidative stress [Fabunmi et al., 1996; Jin et al., 2008]. In the current experiment, superoxide production in the HASMC was quantified by assessing the amount of CM-H_2DCFDA accumulation. Pretreatment with BA significantly suppressed the HG level-induced increase in ROS production. ROS production under HG conditions plays an important role in mediating the specific endogenous tissue inhibitors of MMPs (TIMP)-2 gene expression, accompanied by the regulation of MMP-2 activity [Ho et al., 2007]. With regard to the anti-proliferative effect of BA, at least, it is clear that the BA-induced downregulation of MMPs activity is dependent on the inhibition of ROS production.

A functional NF-κB site has been detected in the proximal stimulatory region of the MMP-9 promoter, and the deletion of this site reduces the upregulation of reporter gene constructs in response to vascular injury [Bond et al., 2001]. The transient overexpression of the inhibitory protein κB-α in VSMC only partially impaired the upregulation of MMP-9, thus suggesting that NF-κB might play a simple permissive role [Yokoo and Kitamura, 1996]. In this study, BA reduced the HG-induced expressions of MMP-2 and MMP-9, as well as p65 NF-κB nuclear translocation, in HASMC. Until now, however, the role played by NF-κB in the upregulation of MMP-2 and MMP-9 remains unclear. Some recent reports have demonstrated that curcumin inhibits osteopontin-induced cell migration,

tumor growth, and NF-κB-mediated MMP-2 activation [Das et al., 2003]. Thus, we suggest that the inhibitory mechanisms of BA might interrupt a signaling cascade involving both the MMP-2 and MMP-9 transcription-mediated activation of NF-κB in HASMC. Thus, further research will be necessary to elucidate the regulatory mechanisms of MMP secretion induced by BA.

Natural products derived from plant sources have been extensively utilized in traditional medicine for the treatment of a myriad of diseases, including cancers and atherosclerosis [Das et al., 2003; Newman et al., 2003; Yoon et al., 2010]. BA is a natural product with a range of biological effects—in particular, BA evidences cholesterol acyltransferase inhibitory activity and vascular anti-inflammatory activity for the treatment of hypercholesterolemia or atherosclerosis [Kwon et al., 2002; Yoon et al., 2010]. In the present study, our hypothesis of the anti-proliferative effect of BA was supported by our findings that BA pretreatment blocked HG-induced [^{3}H]-thymidine incorporation, cell-cycle protein expressions, as well as in vitro invasion and migration in HASMC. Furthermore, ROS/NF-κB signaling was involved in HG-induced activation of both MMP-2 and MMP-9. In conclusion, our results have provided us with a better understanding of the intracellular events activated by HG stimulation and shed new light on the mechanisms by which BA inhibits HG-induced HASMC proliferation and migration. This warrants further exploration of the possible therapeutic uses of BA and other natural products in the regulation of HG-mediated pathological atherosclerosis.

ACKNOWLEDGMENTS

This research was supported by Basic Science Research Program through the National Research Foundation of Korea (NRF) funded by the Ministry of Education, Science and Technology (MEST) (No. R13-2008-028-01000-0), and a grant K10040 to Dr. D.G. Kang funded by Korea Institute of Oriental Medicine.

REFERENCES

Bond M, Chase AJ, Baker AH, Newby AC. 2001. Inhibition of transcription factor NF-kappaB reduces matrix metalloproteinase-1, -3 and -9 production by vascular smooth muscle cells. Cardiovasc Res 50:556–565.

Burggraf D, Trinkl A, Dichgans M, Hamann GF. 2007. Doxycycline inhibits MMPs via modulation of plasminogen activators in focal cerebral ischemia. Neurobiol Dis 25:506–513.

Das R, Mahabeleshwar GH, Kundu GC. 2003. Osteopontin stimulates cell motility and nuclear factor kappaB-mediated secretion of urokinase type plasminogen activator through phosphatidylinositol 3-kinase/Akt signaling pathways in breast cancer cells. J Biol Chem 278:28593–28606.

De Martin R, Hoeth M, Hofer-Warbinek R, Schmid JA. 2000. The transcription factor NF-kB and the regulation of vascular cell function. Arterioscler Thromb Vasc Biol 20:E83–E88.

Fabunmi RP, Baker AH, Murray EJ, Booth RF, Newby AC. 1996. Divergent regulation by growth factors and cytokines of 95 kDa and 72 kDa gelatinases and tissue inhibitors or metalloproteinases-1, -2, and -3 in rabbit aortic smooth muscle cells. Biochem J 315:335–342.

Gabelman BM, Emerman JT. 1992. Effects of estrogen, epidermal growth factor, and transforming growth factor-alpha on the growth of human breast epithelial cells in primary culture. Exp Cell Res 201:113–118.

Golub LM, Lee HM, Ryan ME, Giannobile WV, Payne J, Sorsa T. 1998. Tetracyclines inhibit connective tissue breakdown by multiple non-antimicrobial mechanisms. Adv Dent Res 12:12–26.

Herron GS, Banda MJ, Clark EJ, Gavrilovic J, Werb Z. 1986. Secretion of metalloproteinases by stimulated capillary endothelial cells. II. Expression of collagenase and stromelysin activities is regulated by endogenous inhibitors. J Biol Chem 261:2814–2818.

Ho FM, Liu SH, Lin WW, Liau CS. 2007. Opposite effects of high glucose on MMP-2 and TIMP-2 in human endothelial cells. J Cell Biochem 101:442–450.

Jiang Z, Sui T, Wang B. 2009. Relationships between MMP-2, MMP-9, TIMP-1 and TIMP-2 levels and their pathogenesis in patients with lupus nephritis. Rheumatol Int 30:1219–1226. [Epub ahead of print].

Jin UH, Suh SJ, Chang HW, Son JK, Lee SH, Son KH, Chang YC, Kim CH. 2008. Tanshinone IIA from *Salvia miltiorrhiza* BUNGE inhibits human aortic smooth muscle cell migration and MMP-9 activity through AKT signaling pathway. J Cell Biochem 104:15–26.

Jo M, Thomas LE, Wheeler SE, Curry TE, Jr. 2004. Membrane type 1-matrix metalloproteinase (MMP)-associated MMP-2 activation increases in the rat ovary in response to an ovulatory dose of human chorionic gonadotropin. Biol Reprod 70:1024–1032.

Kwon HJ, Shim JS, Kim JH, Cho HY, Yum YN, Kim SH, Yu J. 2002. Betulinic acid inhibits growth factor-induced in vitro angiogenesis via the modulation of mitochondrial function in endothelial cells. Jpn J Cancer Res 93:417–425.

Lee SO, Jeong YJ, Yu MH, Lee JW, Hwangbo MH, Kim CH, Lee IS. 2006. Wogonin suppresses TNF-alpha-induced MMP-9 expression by blocking the NF-kappaB activation via MAPK signaling pathways in human aortic smooth muscle cells. Biochem Biophys Res Commun 351:118–125.

Lin SJ, Lee IT, Chen YH, Lin FY, Sheu LM, Ku HH, Shiao MS, Chen JW, Chen YL. 2007. Salvianolic acid B attenuates MMP-2 and MMP-9 expression in vivo in apolipoprotein-E-deficient mouse aorta and in vitro in LPS-treated human aortic smooth muscle cells. J Cell Biochem 100:372–384.

Liu B, Bhat M, Nagaraj RH. 2004. αB-crystallin inhibits glucose-induced apoptosis in vascular endothelial cells. Biochem Biophys Res Commun 321:254–258.

Maile LA, Capps BE, Ling Y, Xi G, Clemmons DR. 2007. Hyperglycemia alters the responsiveness of smooth muscle cells to insulin-like growth factor-I. Endocrinology 148:2435–2443.

Matsumoto Y, Park IK, Kohyama K. 2009. Matrix metalloproteinase (MMP)-9, but not MMP-2, is involved in the development and progression of C protein-induced myocarditis and subsequent dilated cardiomyopathy. J Immunol 183:4773–4781.

Newman DJ, Cragg GM, Snader KM. 2003. Natural products as sources of new drugs over the period 1981–2002. J Nat Prod 66:1022–1037.

Orr AW, Sanders JM, Bevard M, Coleman E, Sarembock IJ, Schwartz MA. 2005. The subendothelial extracellular matrix modulates NF-kappaB activation by flow: A potential role in atherosclerosis. J Cell Biol 169:191–202.

Park JM, Kim A, Oh JH, Chung AS. 2007. Methylseleninic acid inhibits PMA-stimulated pro-MMP-2 activation mediated by MT1–MMP expression and further tumor invasion through suppression of NF-kappaB activation. Carcinogenesis 28:837–847.

Piconi L, Quagliaro L, Da Ros R, Assaloni R, Giugliano D, Esposito K, Szabó C, Ceriello A. 2004. Intermittent high glucose enhances ICAM-1, VCAM-1, E-selectin and interleukin-6 expression in human umbilical endothelial cells in culture: The role of poly(ADP-ribose) polymerase. J Thromb Haemost 2:1453–1459.

Ramos-DeSimone N, Hahn-Dantona E, Sipley J, Nagase H, French DL, Quigley JP. 1999. Activation of matrix metalloproteinase-9 (MMP-9) via a converging plasmin/stromelysin-1 cascade enhances tumor cell invasion. J Biol Chem 274:13066–13076.

Ross R. 1993. The pathogenesis of atherosclerosis: A perspective for the 1990s. Nature 362:801–809.

Ruderman NB, Haudenschild C. 1984. Diabetes as an atherogenic factor. Prog Cardiovasc Dis 26:373–412.

Shah PK. 1998. Role of inflammation and metalloproteinases in plaque disruption and thrombosis. Vasc Med 3:199–206.

Sherr CJ. 1996. Cancer cell cycles. Science 274:1672–1677.

Srivastava AK. 2002. High glucose-induced activation of protein kinase signaling pathways in vascular smooth muscle cells: A potential role in the pathogenesis of vascular dysfunction in diabetes. Int J Mol Med 9:85–89.

Suh SJ, Jin UH, Kim SH, Chang HW, Son JK, Lee SH, Son KH, Kim CH. 2006. Ochnaflavone inhibits TNF-alpha-induced human VSMC proliferation via regulation of cell cycle, ERK1/2, and MMP-9. J Cell Biochem 99:1298–1307.

Wassmann S, Wassmann K, Nickenig G. 2006. Regulation of antioxidant and oxidant enzymes in vascular cells and implications for vascular disease. Curr Hypertens Rep 8:69–78.

Xu P, Wang YL, Zhu SJ, Luo SY, Piao YS, Zhuang LZ. 2000. Expression of matrix metalloproteinase-2, -9, and -14, tissue inhibitors of metalloproteinase-1, and matrix proteins in human placenta during the first trimester. Biol Reprod 62:988–994.

Yao JS, Chen Y, Zhai W, Xu K, Young WL, Yang GY. 2004. Minocycline exerts multiple inhibitory effects on vascular endothelial growth factor-induced smooth muscle cell migration: The role of ERK1/2, PI3K, and matrix metalloproteinases. Circ Res 95:364–371.

Yasunari K, Kohno M, Kano H, Yokokawa K, Minami M, Yoshikawa J. 1997. Mechanisms of action of troglitazone in the prevention of high glucose-induced migration and proliferation of cultured coronary smooth muscle cells. Circ Res 81:953–962.

Yokoo T, Kitamura M. 1996. Dual regulation of IL-1 beta-mediated matrix metalloproteinase-9 expression in mesangial cells by NF-kappa B and AP-1. Am J Physiol 270:F123–F130.

Yoon JJ, Lee YJ, Kim JS, Kang DG, Lee HS. 2010. Protective role of betulinic acid on TNF-alpha-induced cell adhesion molecules in vascular endothelial cells. Biochem Biophys Res Commun 391:96–101.